

# BioSim Incubator: A Non-Biological Egg Incubation Simulation Platform

Rapinpa Rasnidatta<sup>1\*</sup> and Pitikhate Sooraksa<sup>2</sup>

<sup>1</sup>Krutoo Home Education, Charn Issara Tower 1, Rama IV Rd, Suriya Wong, Bang Rak, Bangkok, 10500, Thailand

<sup>2</sup>Department of Robotics and AI, School of Engineering, King Mongkut's Institute of Technology Ladkrabang,  
1 Chalongkrung 1, Ladkrabang, Bangkok, 10520, Thailand

(Received September 30, 2025; accepted October 10, 2025)

**Keywords:** BioSim, non-biological egg, egg incubation, simulation platform

This study presents the design, development, and evaluation of a BioSim incubator that integrates IoT-based environmental control with a biosimulation framework for predicting embryo development. The system employed an ESP8266 microcontroller, an SHT30 sensor, and a Node-RED/MQTT architecture to enable the real-time monitoring, automated actuation, and feedback control of temperature, humidity, and airflow. Experimental trials replicated the two key incubation stages: the development stage (Days 1–18,  $37.5 \pm 0.2$  °C, 50–55% RH) and the lockdown stage (Days 19–21,  $37.5 \pm 0.2$  °C, 65–70% RH). Results showed that the incubator maintained stable conditions within biologically favorable ranges, with only minor fluctuations that were rapidly corrected by the control logic. Comparison with practical risk guidelines indicated that the incubator's performance corresponded predominantly to the “guaranteed survival” zone. To extend evaluation beyond environmental parameters, a virtual embryo feedback system was implemented as part of the BioSim framework, mapping deviations in temperature and humidity to predicted biological outcomes, which consistently indicated healthy chick development. In addition to demonstrating technical feasibility, the BioSim incubator provides a safe and accessible tool for STEM education and training, allowing students to study the relationship between environmental control and biological development without the use of live eggs.

## 1. Introduction

Thailand has long had an economic base rooted in agriculture, particularly in rural areas where animal husbandry for household consumption and community sales is widespread. Raising chickens for egg production and incubation is a common activity in nearly every region. Traditionally, incubation relied on natural brooding, where hens provided warmth and protection until hatching. While simple and low-cost, this method has several limitations: hatchability varies with season, temperature, humidity, and farmer expertise. According to the Department of Livestock Development, natural hatching rates average 70–80% under favorable conditions

---

\*Corresponding author: e-mail: [nanarapinpa@gmail.com](mailto:nanarapinpa@gmail.com)  
<https://doi.org/10.18494/SAM5951>

but may fall below 50% in hot, rainy, or disturbed environments.<sup>(1)</sup> Such fluctuations reduce farmer income and limit the stability of chick supply.

Artificial incubation was developed to overcome these limitations by controlling environmental variables independently of climate or season. Modern incubators regulate temperature, humidity, ventilation, and egg turning using sensors, microcontrollers, and actuators, thereby improving efficiency, reducing mortality, and increasing consistency. Optimal incubation conditions are well established: 37–38 °C and 50–55% relative humidity (RH) with regular egg turning for days 1–18, and 65–70% RH without turning during the final three days (lockdown).<sup>(2,3)</sup>

Several studies demonstrate that even simple systems can achieve high hatchability. Al-Zaidi emphasized thermal design with thick insulation, achieving 98.39% hatchability at 37.5 °C.<sup>(3)</sup> Mohlalisi *et al.* employed proportional-integral-derivative (PID) temperature control and automatic humidity adjustment, maintaining 36.9–39.0 °C and 35–75% RH.<sup>(4)</sup> Idoko *et al.* achieved incubation conditions of  $37 \pm 1$  °C and ~58% RH (70% lockdown), noting fewer incubation losses, but the hatchability rate was not reported.<sup>(5)</sup>

Internet of Things (IoT) technologies further enhance control and monitoring. Panumonwatee *et al.* improved hatchability from 61 to 76% by maintaining 37.5 °C and 55–60% RH (days 1–18), and 36.5–37.2 °C and 65–70% RH (days 19–21).<sup>(6)</sup> Poolwan *et al.* maintained 37.8 °C/60% RH and 37.5 °C/70% RH, supporting ~80% hatchability.<sup>(7)</sup> Jusman *et al.* reported 91% hatchability at 37–40 °C and 55–60% RH. Wahyuni *et al.* applied fuzzy logic control, achieving stable 37.7–38.8 °C and 57–67% RH with high user satisfaction.<sup>(8,9)</sup>

Recent works integrate advanced filtering or control schemes. Dilip *et al.* combined ESP8266 microcontrollers with Kalman filtering, achieving 88.9% hatchability at  $37.5 \pm 0.2$  °C and 50–70% RH. Kone *et al.* used an ESP32 system to maintain 37–38 °C and 45–60% RH with automatic turning, demonstrating stable environmental control.<sup>(10,11)</sup> Tangsuknirundorn *et al.* developed a STEM-based cyber-physical incubator using Arduino control, DHT22 sensor, and Kalman filtering to maintain 37.5 °C and 58% RH during incubation, demonstrating effective environmental regulation and strong educational outcomes.<sup>(12)</sup>

Kocher and Izadeen reviewed 21 microcontroller-based designs, recommending 37.5 °C and 25–60% RH followed by 70–80% RH near hatch. Zakaria *et al.* conducted a systematic review, highlighting PID as superior to on/off control, with hatchability reaching ~92%.<sup>(13,14)</sup>

Energy constraints have motivated resilient designs. Peprah *et al.* developed a GSM/IoT-enabled solar incubator that maintained 37.5 °C and 50–70% RH, achieving hatchability above 95% in multiple trials.<sup>(15)</sup>

Taken together, these studies consistently demonstrate that maintaining ~37.5 °C, 50–55% RH (days 1–18), and 65–70% RH (days 19–21), coupled with regular egg turning, yields the highest hatchability. Control strategies range from simple on/off relays to PID and fuzzy logic, with IoT increasingly providing real-time monitoring and remote control.

However, most aforementioned studies focus only on biological outcomes such as hatchability and chick survival, with limited emphasis on simulation-based tools for design testing and education. To address this gap, this study introduces the BioSim Incubator, a non-biological

simulation platform that reproduces incubation dynamics for engineering evaluation, educational purposes, and design optimization.

## 2. Materials and Methods

### 2.1 Biosim incubator design

The BioSim Incubator is a simulation-based smart incubator that integrates IoT sensors, microcontroller control, and a virtual embryo feedback model. Unlike conventional systems, it does not use live eggs; instead, it maps environmental parameters—temperature, humidity, ventilation, and turning—to simulated embryonic development. This approach makes testing ethical, cost-effective, and repeatable, enabling early troubleshooting, rapid optimization, and reduced development time. Designed as both a research and educational tool, the BioSim Incubator supports best-practice development and advances the understanding of incubation processes. Figure 1 shows an in-house BioSim Incubator designed and implemented by the authors. The incubator chamber was used as a testbed in this study.

According to Fig. 1, heating was provided by two 60 W incandescent bulbs mounted in the middle of the box to ensure a uniform thermal distribution, while two DC exhaust fans were positioned near the upper wall to facilitate air exchange and prevent heat or humidity buildup. A shallow water tray was placed at the bottom of the chamber to act as a passive humidifier, with a large surface area adjusted to meet the target humidity range. An egg-turning mechanism was installed centrally to enable the regular tilting of eggs at approximately 45°, preventing embryonic adhesion.

### 2.3 Hardware and connectivity system

In this research, an automatic egg incubator control system was designed and developed using the following main components: the ESP8266 NodeMCU Development board (hereafter

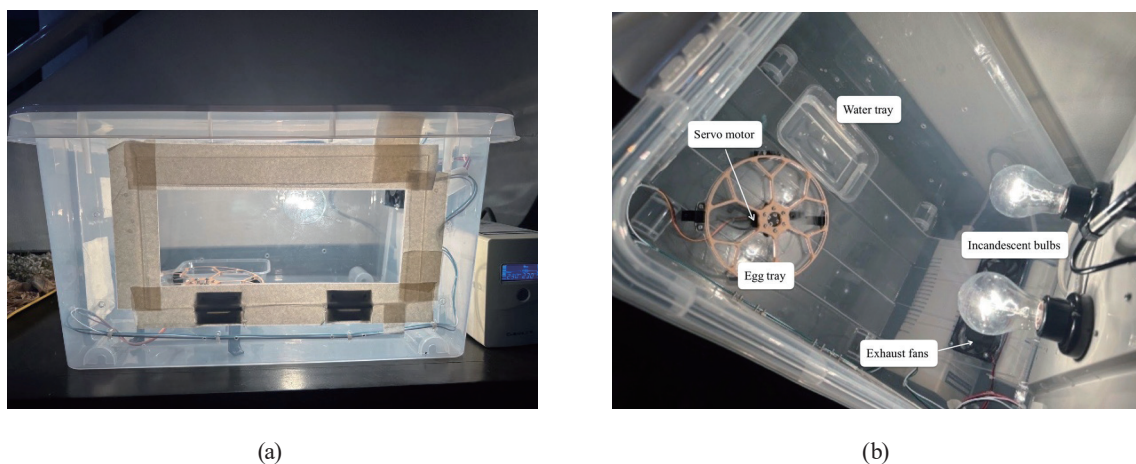


Fig. 1. (Color online) Incubator chamber.

referred to as ESP8266 NodeMCU), the MQTT communication protocol, a Node-RED control dashboard, and a central server for data processing and storage.

### 2.3.1 ESP8266 NodeMCU

The ESP8266 NodeMCU served as the central microcontroller of the BioSim Incubator, handling environmental monitoring and device actuation through a closed-loop control algorithm. The connected components are as follows.

- Two exhaust fans — remove excess heat and humidity
- Two 60 W incandescent bulbs (E27 sockets) — heating source
- Servo motor — egg turning
- SHT31 sensor — temperature and humidity sensing

The system architecture is summarized in Fig. 2, showing how the ESP8266 NodeMCU interfaces with sensors, actuators, and relays.

### 2.3.2 Communication protocol (MQTT)

The system employed the Message Queuing Telemetry Transport (MQTT) protocol for lightweight publish/subscribe communication. The ESP8266 NodeMCU, programmed with predefined control thresholds, functioned as the primary controller. It read temperature and humidity values from the SHT30 sensor, executed the control logic, and directly issued commands to actuators (heating bulbs, fans, humidifier, and servo motor). At the same time, the ESP8266 NodeMCU operated as an MQTT client, publishing sensor data to topics (e.g., TEMP\_TOPIC, HUMIDITY\_TOPIC) for logging and visualization. A local computer hosted the MQTT broker and Node-RED dashboard, which subscribed to these topics to display real-time data and enable user supervision. This configuration ensured reliable two-way communication,

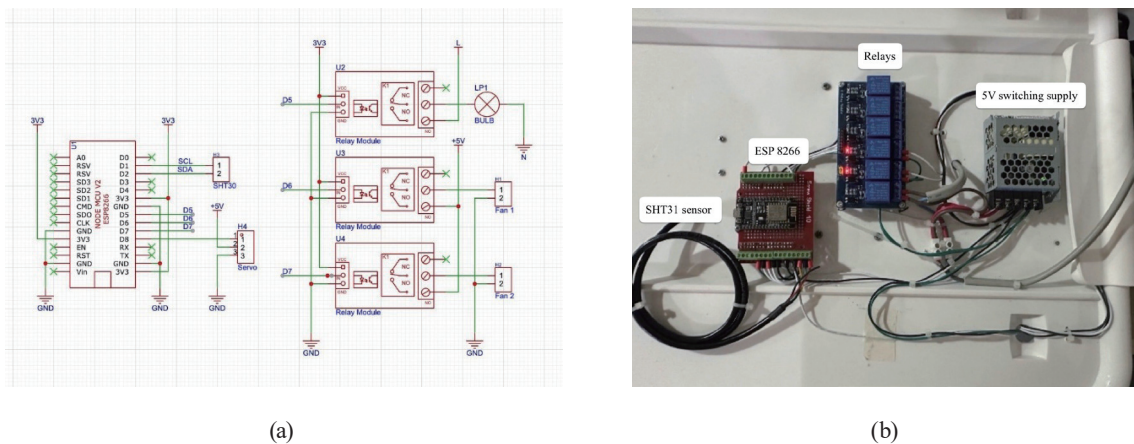


Fig. 2. (Color online) Circuit schematic and wiring of the BioSim Incubator showing the ESP8266 NodeMCU interfacing with the SHT31 sensor, servo motor, heating bulbs, fans, and relays.

supporting the autonomous operation of the incubator while allowing supervisory monitoring and manual override via Node-RED.

2.3.3 Node-RED dashboard and data visualization

Node-RED was used to build the graphical dashboard for supervisory control and data visualization. The dashboard displayed real-time sensor readings (temperature and humidity) and actuator status (heating bulbs, fans, humidifier, and servo motor), and also stored data for historical trend analysis. Users could manually intervene through the interface by publishing override commands to the ESP8266 NodeMCU, for example, forcing an actuator ON or OFF, but under normal operation, the ESP8266 NodeMCU executed control autonomously according to its programmed thresholds. This arrangement ensured that incubation could continue independently of the server while still providing user flexibility, monitoring, and logging functions. A sample dashboard layout is shown in Fig. 3.

2.3.4 Data logging and analysis via MQTT

Data from the ESP8266 NodeMCU were continuously published to the MQTT broker hosted on the central server. Node-RED subscribed to these topics, processed the incoming data, and stored them in a local database for long-term recording. The stored values were visualized as time-series graphs on the Node-RED dashboard, enabling both the real-time monitoring and retrospective evaluation of environmental stability. While ESP8266 NodeMCU was responsible for the direct control of actuators, Node-RED provided supervisory oversight, allowing performance assessment and optional manual adjustments through the dashboard.

2.4 Implemented control algorithm

The ESP8266 NodeMCU executed a closed-loop algorithm to regulate temperature, humidity, and egg turning based on user-defined setpoints from the Node-RED dashboard. Temperature was maintained within  $\pm 0.2\text{ }^{\circ}\text{C}$  of the target by switching heating bulbs on/off. Humidity control adapted to the incubation stage:  $\pm 5\%$  RH during days 1–18 and  $+10\%$  RH threshold during days 19–21. Egg turning occurred every 6 h until day 18 and was disabled thereafter. The decision flowchart is provided in Appendix A.

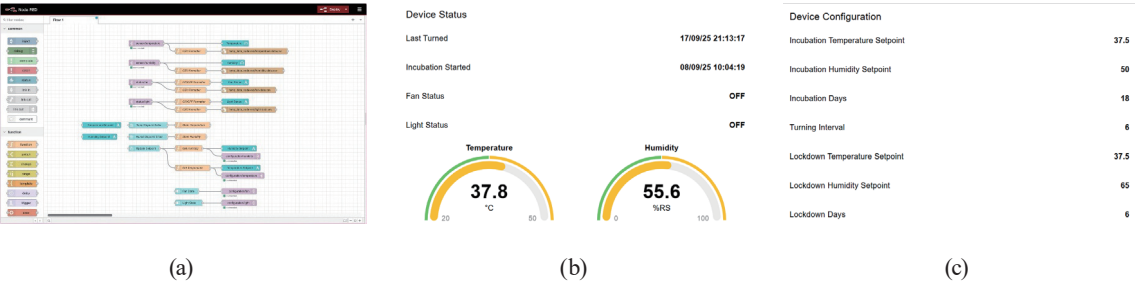


Fig. 3. (Color online) (a) Node-RED flow for data acquisition and control logic. (b) Dashboard interface showing real-time temperature, humidity, actuator status, and adjustable setpoints.

3. Experimental Results and Discussion

3.1 Experimental design

Two incubation stages were simulated on the basis of the established biological requirements. Table 1 provides control specifications for both the development and lockdown stages. In the development stage (days 1–18), the set-point temperature and relative humidity were  $37.5 \pm 0.2$  °C and 50–55% RH respectively, with scheduled egg turning, while in the lockdown stage (days 19–21), the set-points were  $37.5 \pm 0.2$  °C and 65–70% RH, with turning disabled to allow chicks to position for hatching. The egg tray was mounted on a servo-driven mechanism programmed to tilt every 6 h during the development stage, corresponding to 3–4 turns per day, which aligns with common incubation practice. Turning was automatically disabled during the lockdown stage. The  $\pm 0.2$  °C tolerance was chosen to minimize thermal stress while remaining achievable with incandescent heating and fan-based ventilation.

3.2 Practical guidelines for evaluating risk levels under different incubation temperature and humidity conditions

The recorded environmental conditions during testing are presented in Fig. 4. The temperature profile remained consistently stable at  $37.5 \pm 0.2$  °C, within the optimal range for incubation. Relative humidity was maintained between 52 and 62% RH, which matched the requirements of the development stage (50–55% RH) and approached the target for the lockdown stage (65–70% RH). Minor short-lived fluctuations above 55% RH were observed but gradually stabilized within 3–5 min owing to the passive water tray system, where evaporation adjusted the chamber moisture level. Importantly, no instances of extreme conditions were recorded, such as humidity below 48% RH or temperature above 37.7 °C.

Table 1  
Experimental setpoints for simulated incubation stages.

Stage	Days	Temperature (°C)	Humidity (%)	Turning
Development	1–18	$37.5 \pm 0.2$	50–55	Every 6 h
Lockdown	19–21	$37.5 \pm 0.2$	65–70	Disabled

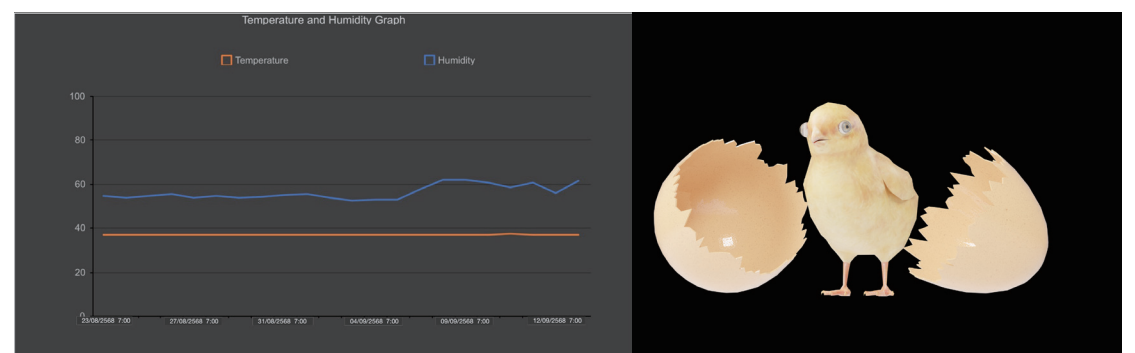


Fig. 4. (Color online) Temperature and humidity profiles recorded during incubation.

Experimental results demonstrated that the incubator consistently maintained temperature at  $37.5 \pm 0.2$  °C and humidity within the biologically required ranges of 50–55% RH during the development stage and 65–70% RH during the lockdown stage. When evaluated against practical risk guidelines, the incubator’s performance corresponded predominantly to the “guaranteed survival” zone, with only minor and rapidly corrected deviations into moderate-risk ranges. A virtual embryo feedback model further validated the biological relevance of the recorded conditions, predicting healthy chick development under the maintained environment.

To interpret these results, Table 2 shows practical guidelines from the literature<sup>(16–20)</sup> that categorize different combinations of temperature and humidity into risk levels. The optimal environment—37.3–37.7 °C with 48–52% RH—is associated with “guaranteed survival”, while deviations introduce risks such as dehydration, delayed development, weak chicks, or suffocation.

When compared with these guidelines, the experimental results correspond primarily to the “guaranteed survival” zone. Occasional short excursions into the ‘moderate risk’ humidity range (above 52% RH during early development) briefly indicated the potential for hatching difficulty but were too short-lived to affect outcomes. Rapid recovery ensured that the incubation process remained stable and within safe limits.

Overall, the combination of Table 2 and Fig. 4 confirms that the IoT-based incubator successfully sustained a biologically favorable environment throughout the experimental period. The integration of Node-RED real-time monitoring with automated feedback control provided both stability and reliability, validating the system’s capability to support healthy embryo development and successful lockdown stage.

Table 2  
Risk levels for embryo development under different incubation temperature and humidity conditions.

Temperature	Humidity	Result	Explanation
Low (<37.3 °C)	Low (<48%)	Fatal risk	Too cold & too dry → embryo underdeveloped/dehydration <sup>(16,17)</sup>
Low (<37.3 °C)	Optimal (48–52%)	Slight risk	Low temperature → possible incomplete development <sup>(18)</sup>
Low (<37.3 °C)	High (>52%)	Risk	Cold & too humid → slow hatching, weak chick, labored breathing <sup>(16)</sup>
Optimal (37.3–37.7 °C)	Low (<48%)	Moderate risk	Inappropriate humidity → hatching difficulty <sup>(16,19)</sup>
Optimal (37.3–37.7 °C)	Optimal (48–52%)	Guaranteed survival	Balance environment <sup>(16,20)</sup>
Optimal (37.3–37.7 °C)	High (>52%)	Moderate risk	Inappropriate humidity → hatching difficulty <sup>(16,20)</sup>
Low (>37.7 °C)	Low (<48%)	Risk	Too hot & too dry → dehydration/hard shell <sup>(17,19)</sup>
Low (>37.7 °C)	Optimal (48–52%)	Slight risk	High temperature → rapid development, early hatching <sup>(16,18)</sup>
Low (>37.7 °C)	High (>52%)	Fatal risk	Too hot & too humid → suffocation/drowning <sup>(16,17,19)</sup>

### 3.3 Virtual embryo feedback for evaluation

Although the incubator successfully maintained stable environmental conditions, direct testing with fertile eggs was not conducted during this stage. To compensate for this limitation and to assess the biological implications of the measured temperature and humidity profiles, a virtual embryo feedback system was developed. This system served as a simulation framework to predict chick developmental outcomes under various incubation environments.

The virtual embryo feedback model was based on heuristic mapping, where deviations from optimal temperature and humidity setpoints were linked to specific biological outcomes. For example, prolonged exposure to low humidity conditions ( $<48\%$  RH) was mapped to embryo dehydration and hardened shells, while excessive humidity ( $>52\%$  RH) predicted weak chicks, labored breathing, or drowning during hatching. Similarly, sub-optimal temperatures ( $<37.3\text{ }^{\circ}\text{C}$  or  $>37.7\text{ }^{\circ}\text{C}$ ) were associated with incomplete development, premature hatching, or suffocation, depending on the magnitude of deviation.

When the recorded experimental data (Fig. 4) were applied to this virtual embryo model, the outcomes consistently mapped to the “healthy chick” pathway under optimal conditions. Occasional short excursions into moderate-risk humidity zones briefly triggered branches toward “hatching difficulty” outcomes, but these were corrected once the incubator stabilized, returning the model output to the healthy development pathway.

This approach provided a means of validating the incubator’s performance in the absence of live biological trials. By linking environmental stability to predicted developmental outcomes, the virtual embryo feedback system confirmed that the IoT-controlled incubator was capable of sustaining conditions necessary for successful embryo development and hatching, consistent with the risk thresholds outlined in Table 2. A summary of these mapped relationships is illustrated in Fig. 5,

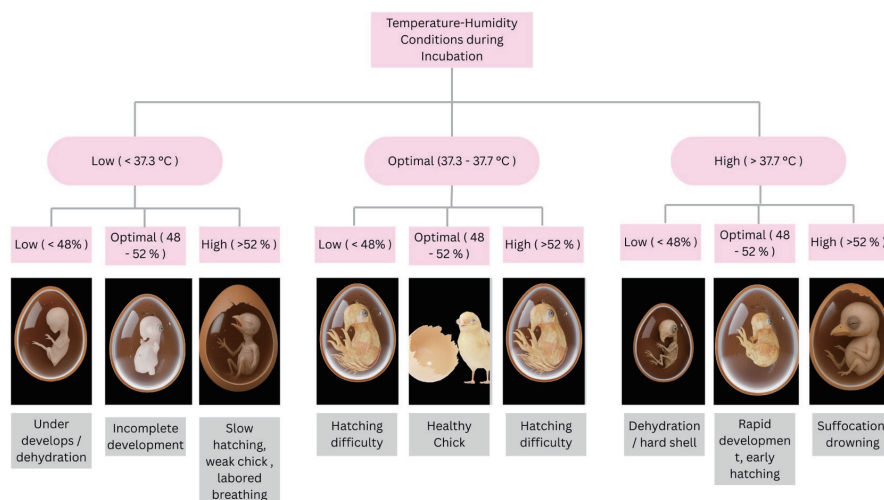


Fig. 5. (Color online) Tree diagram of the virtual embryo feedback system. Environmental conditions (temperature and humidity) are mapped to developmental outcomes, ranging from a healthy chick under optimal conditions to various failure modes under adverse conditions.

which links combinations of temperature-humidity conditions to the corresponding predicted developmental outcomes.

### 3.4 Design challenges and implemented solutions

During testing, several design challenges were identified and addressed through iterative modifications. Excessive airflow from the initial fan configuration caused rapid drops in temperature and humidity; this was resolved by reducing the setup to two exhaust fans, which provided adequate ventilation without destabilizing conditions. The DHT11 sensor was replaced with a more accurate SHT30 sensor to eliminate fluctuations in measurement. Large intake openings allowed uncontrolled external air exchange, making the chamber highly sensitive to ambient conditions; sealing these openings and replacing them with smaller perforations reduced losses of heat and humidity while preserving passive gas exchange.

Humidity control also requires refinement. An ultrasonic humidifier produced unstable and excessive humidity, so it was replaced with a passive water tray system, where the surface area of exposed water governed gradual and stable humidification. On the control side, limitations of the Blynk platform in flexibility and data handling were overcome by migrating to a Node-RED and MQTT environment, which enabled advanced customization and real-time visualization. Finally, location tests showed that operating the incubator in an air-conditioned room led to persistently low humidity due to dry background air and that relocating the system to a naturally humid space significantly improved stability. These modifications collectively enhanced the reliability of environmental regulation within the incubator, ensuring more uniform and biologically favorable conditions.

Design challenges such as unstable airflow, sensor inaccuracies, excessive humidification, and platform limitations were systematically identified and resolved through iterative modifications. These improvements enhanced the stability and reliability of the system, confirming its capability to maintain uniform incubation conditions even under various environmental effects.

In addition to demonstrating the technical feasibility of low-cost IoT integration, this work makes two broader contributions:

1. Advancement of incubation technology — by introducing a flexible, modular, and remotely monitored control architecture, the incubator expands the potential of smart farming and educational applications.
2. Support for embryo developmental studies — by combining environmental monitoring with a virtual embryo feedback model, the system provides a novel framework for linking engineering parameters with predicted biological outcomes, even in the absence of live testing.

## 4. Conclusions

This study presented the design, development, and evaluation of an IoT-based egg incubator capable of regulating temperature, humidity, and airflow with integrated monitoring and control.

The system employed an ESP8266 NodeMCU microcontroller, an SHT30 sensor, and a Node-RED/MQTT architecture to achieve real-time data visualization, automated actuation, and reliable feedback control.

Overall, the developed incubator demonstrates the feasibility of integrating IoT technologies into low-cost, small-scale hatching systems. Its modular design, real-time monitoring, and automated control functions make it adaptable for both educational and smallholder farming applications. Future work will involve field testing with fertile eggs under farm conditions, implementing an advanced control strategy such as PID or fuzzy logic, and exploring predictive analytics to further optimize hatching performance.

### Acknowledgments

The authors acknowledge Nonpawit Ekburanawat of the KMITL Interactive Digital Center for evaluating the egg incubator and providing valuable suggestions. Financial support from the family of the first author is also gratefully acknowledged.

### References

- 1 S. Janram and B. Chutimantanon: Kanchanaburi Provincial Livestock Office (2018). [https://pvlo-knr.dld.go.th/webfile/study/Factors\\_Affecting.pdf](https://pvlo-knr.dld.go.th/webfile/study/Factors_Affecting.pdf)
- 2 G. S. Archer and A. L. Cartwright: Texas A&M AgriLife Ext. Serv. Publ. E-635 (2013) 13. <https://poultry.tamu.edu/wp-content/uploads/sites/14/2023/07/E-635-Hatching-Eggs-in-the-Classroom-A-Teachers-Guide.pdf>
- 3 A. A. M. A. Al-Zaidi: Technium **4** (2022) 1. <https://www.researchgate.net/publication/360033769>
- 4 S. Mohlalisi, T. Koetje, and T. Thamae: Smart Agric. Technol. **7** (2024) 100387. <https://doi.org/10.1016/j.atech.2023.100387>
- 5 E. Idoko, G. O. Ogbeh, and F. T. Ikule: Int. J. Innov. Res. Multidiscip. Field **5** (2019) 1. <https://www.researchgate.net/publication/334459889>
- 6 G. Panumonwatee, N. Preecha, and S. Choosumrong: J. Appl. Res. Sci. Technol. **21** (2022) 79. <https://doi.org/10.14456/jarst.2022.19>
- 7 J. Poolwan, B. Sripan, and S. Kingthong: RMUTSB Acad. J. **9** (2021) 225. <https://li01.tci-thaijo.org/index.php/rmutsb-sci/article/download/249695/173078>
- 8 Y. Jusman, M. I. Kusumabrata, K. Purwanto, and M. A. F. Nurkholid: E3S Web Conf. **570** (2024) 01010. <https://doi.org/10.1051/e3sconf/202457001010>
- 9 R. Wahyuni, Y. Irawan, A. Febriani, Nurhadi, and H. T. Saputra: Ilkom J. Comput. Sci. **19** (2024) 134. <https://www.researchgate.net/publication/384439442>
- 10 T. Dilip, K. G. Hegde, N. S. Naveena, and S. B. N. Sumanth: CMR Inst. Technol. Proj. Rep. (2020). <https://www.researchgate.net/publication/352777744>
- 11 T. Koné, N. G. Anoh, B. G. Yatanan, Y. A. A. Brou, N. J. Ahoutou, and J. D. A. Allou: Eng. Technol. J. **9** (2024) 396. <https://everant.org/index.php/etj/article/view/1162/812>
- 12 P. Tangsuknirundorn and P. Sooraksa: Proc. 5th Int. Conf. Eng. Appl. Sci. Technol. (ICEAST 2019) (IEEE, Thailand, 2019) 382. <https://doi.org/10.1109/ICEAST.2019.8802564>
- 13 I. S. H. Kocher and G. Y. Izadeen: Acad. J. Nawroz Univ. **11** (2022) 139. <https://www.researchgate.net/publication/365107606>
- 14 D. Zakaria, M. B. Hamzah, D. S. Nazhif, M. H. Muttaqin, M. R. Wahid, R. B. Prayudha, A. Ramelan, and A. Nugraha: J. Electr. Electron. Inf. Commun. Technol. **5** (2023) 33. <https://doi.org/10.20961/jeeict.5.1.72718>
- 15 F. Peprah, S. Gyamfi, M. Amo-Boateng, E. Buadi, and M. Obeng: Sci. Afr. **17** (2022) e01326. <https://doi.org/10.1016/j.sciaf.2022.e01326>
- 16 H. G. Barott: Poult. Sci. **16** (1937) 311. <https://www.hatchability.com/Barott.pdf>
- 17 R. M. Noiva, C. Menezes, and J. A. Peleteiro: Poult. Sci. **93** (2014) 2394. <http://www.biomedcentral.com/1746-6148/10/234>

- 18 S. Yalcin, S. Özkan, and T. Shah: *Front. Physiol.* **13** (2022) 899977. <https://doi.org/10.3389/fphys.2022.899977>  
19 M. M. Adame and N. Ameha: *Asian J. Biol. Sci.* **16** (2023) 474. <https://doi.org/10.3923/ajbs.2023.474.484>  
20 Poultry Hub: <https://www.poultryhub.org/anatomy-and-physiology/incubation> (accessed September 2025).

## About the Authors



**Rapinpa Rasmidatta** is a Year 13 student at Krutoo Home Education with a strong academic interest in engineering, technology, and STEM education. She previously founded the Girls Who Code Club at Bangkok Prep International School, where she had promoted coding among younger students. Her research interests include IoT systems, smart devices, and applications of engineering to support education and sustainable development. She is also an active advocate for women in STEM, aiming to inspire greater female participation in science and technology fields.

([nanarapinpa@gmail.com](mailto:nanarapinpa@gmail.com))



**Pitikhate Sooraksa** is a professor at the School of Engineering, King Mongkut's Institute of Technology Ladkrabang, Thailand. He received his B.Ed. (Hons) and M.Sc. degrees in physics from Srinakharinwirot University, Thailand, his M.S. degree from George Washington University, USA, in 1992, and his Ph.D. degree from the University of Houston, USA, in 1996, both in electrical engineering. His research interests include cyber-physical applications and rapid prototypes in robotics and AI.

([pitikhate.so@kmitl.ac.th](mailto:pitikhate.so@kmitl.ac.th))

## Appendix A

The control logic flowchart used in the experiment can be illustrated in Fig. A1.

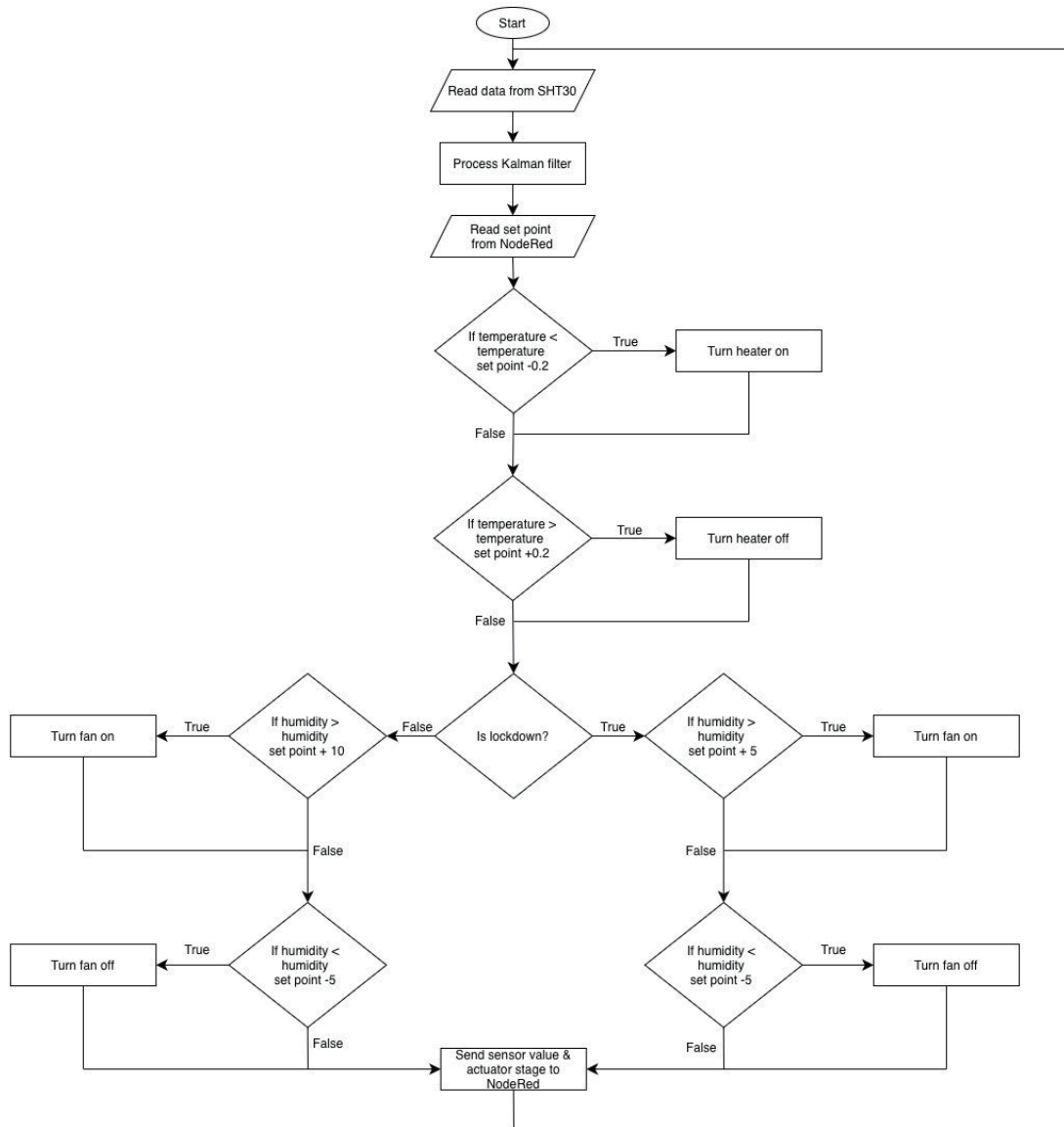


Fig. A1. Control logic flowchart of the ESP8266 NodeMCU showing threshold-based regulation and lockdown.